

CFD SIMULATION OF VORTEX-INDUCED  
VIBRATION OF A BLUFF BODY STRUCTURE BY  
ANSYS FLUENT

ABDUL HALIM BIN ABDUL RAHMAN

A project report submitted in partial  
fulfillment of the requirement for the award of the  
Degree of Master of Mechanical Engineering

Faculty of Mechanical and Manufacturing Engineering  
Universiti Tun Hussein Onn Malaysia

JULY 2015

## **Abstract**

Vortex-induced vibration is a vibration phenomenon which occurred to the bluff body structure either on the ground or sea underneath. The investigations of the effect of flow velocity on the transverse vibration of bluff body were done to determine the vortex shedding frequency for each of the analyses. Besides it was also to investigate the flow velocity and pressure loss in the time response. Despite the investigation made by other researchers, a study on a very high turbulence Reynolds number, were still blurred unknown. In response to this problem, this study is purposely to investigate at a very high Reynolds number and simulated through ANSYS Fluent software's which started from a minimum of 70 000 Reynolds number and increased to the maximum of 350 000 Reynolds number. A one meter in diameter of cylindrical aluminium was used for the study where the velocity was in cross-flow direction. From the simulated results, it could be seen the fluid flow after the boundary layer was an asymmetric flow. The Strouhal number seems to be decreased by the increase of Reynolds number while the frequencies were increased with the increased of Reynolds number.

## **Abstrak**

Getaran disebabkan vorteks (VIV) adalah satu fenomena getaran yang berlaku kepada struktur badan tumpul samada di tanah atau di bawah laut. Kajian terhadap kesan halaju aliran pada getaran melintang badan tumpul telah dilakukan untuk menentukan frekuensi penumpahan vorteks bagi setiap analisis. Selain itu tujuan penyelidikan ini juga dalah untuk menyiasat halaju aliran dan kehilangan tekanan didalam tindak balas masa. Walaupun terdapat penyelidikan yang dibuat oleh penyelidik lain, kajian mengenai pergolakan nombor Reynolds yang sangat tinggi, masih kabur dan tidak diketahui. Untuk menjawab permasalahan ini, kajian ini bertujuan untuk menyiasat dengan nombor Reynolds yang sangat tinggi melalui simulasi perisian ANSYS Fluent yang bermula dari minimum 70 000 nombor Reynolds dan meningkat kepada maksimum 350 000 nombor Reynolds.. Satu selinder aluminium yang bergaris pusat satu meter telah digunakan dalam kajian ini di mana halaju aliran adalah dalam arahan merentas selinder. Hasil dari keputusan simulasi, dapat dilihat cecair yang mengalir melepasi lapisan sempadan adalah aliran tidak simetri. Nombor Strouhal kelihatan menu-run apabila nombor Reynolds meningkat, manakala frekuensi pula meningkat dengan peningkatan nombor Reynolds.

# Contents

<b>Declaration</b>	<b>iii</b>
<b>Dedication</b>	<b>iv</b>
<b>Acknowledgment</b>	<b>v</b>
<b>Abstract</b>	<b>vi</b>
<b>Abstrak</b>	<b>vii</b>
<b>List of Figures</b>	<b>xi</b>
<b>List of Tables</b>	<b>xii</b>
<b>List of Appendices</b>	<b>xiii</b>
<b>List of Symbols</b>	<b>xv</b>
<b>1 Introduction</b>	<b>1</b>
1.1 Background of Study	1
1.1.1 Vortex-Induced Vibration	2
1.1.2 Bluff Body	2
1.1.3 Computational Fluid Dynamics (CFD)	3
1.2 Problem Statement	3
1.3 Objective of the Study	3
1.4 Scopes of the Study	4
<b>2 Literature Review</b>	<b>5</b>
2.1 Reynolds Number	6
2.2 Strouhal Number	6
2.3 Effect of Flow Velocity	7
2.4 Vortex Shedding	7

2.5	Previous Research	8
<b>3</b>	<b>Methodology</b>	<b>11</b>
3.1	Numerical Study	11
3.2	Physical Model	12
3.3	Numerical Methods	13
3.3.1	Finite Volume Method	14
3.3.2	Finite Element Method	14
3.3.3	Finite Difference Method	14
3.4	Governing Equations	15
3.5	Boundary Conditions	18
3.6	Computational Fluid Dynamics	18
3.6.1	Preprocessing	19
3.6.2	Solver	20
3.6.3	Post Processing	20
3.7	Methodology Summary	20
<b>4</b>	<b>RESULTS AND DISCUSSION</b>	<b>22</b>
4.1	Validation	22
4.2	Velocity Magnitude	23
4.3	Vorticity Magnitude	28
4.4	Pressure Coefficient	32
4.5	Strouhal Number	37
4.6	Frequency of Vortex Shedding	40
<b>5</b>	<b>CONCLUSIONS AND RECOMMENDATIONS</b>	<b>42</b>
	<b>References</b>	<b>43</b>

## List of Figures

2.1	Cylinder arrangement in the wind tunnel	9
3.1	Schematic diagram of the flow field around circular cylinder [7]	13
3.2	Steps Performed in CFD	19
3.3	Flowchart of Methodology	21
4.1	Trending line validation between present study and Simmons	23
4.2	Contours of Velocity Magnitude at Re=70000	24
4.3	Vectors of Velocity Magnitude at Re=70000	24
4.4	Contours of Velocity Magnitude at Re=150000	24
4.5	Vectors of Velocity Magnitude at Re=150000	25
4.6	Contours of Velocity Magnitude at Re=200000	25
4.7	Vectors of Velocity Magnitude at Re=200000	25
4.8	Contours of Velocity Magnitude at Re=250000	26
4.9	Vectors of Velocity Magnitude at Re=250000	26
4.10	Contours of Velocity Magnitude at Re=300000	26
4.11	Vectors of Velocity Magnitude at Re=300000	27
4.12	Contours of Velocity Magnitude at Re=350000	27
4.13	Vectors of Velocity Magnitude at Re=350000	27
4.14	Contours of Vorticity Magnitude at Re=70000	28
4.15	Vectors of Vorticity Magnitude at Re=70000	28
4.16	Contours of Vorticity Magnitude at Re=150000	29
4.17	Vectors of Vorticity Magnitude at Re=150000	29
4.18	Contours of Vorticity Magnitude at Re=200000	29
4.19	Vectors of Vorticity Magnitude at Re=200000	30
4.20	Contours of Vorticity Magnitude at Re=250000	30
4.21	Vectors of Vorticity Magnitude at Re=250000	30
4.22	Contours of Vorticity Magnitude at Re=300000	31
4.23	Vectors of Vorticity Magnitude at Re=300000	31
4.24	Contours of Vorticity Magnitude at Re=350000	31

4.25	Vectors of Vorticity Magnitude at Re=350000	32
4.26	Vectors of Pressure Coefficient at Re=70000	33
4.27	Pressure Coefficient around cylinder at Re=70000	33
4.28	Vectors of Pressure Coefficient at Re=150000	33
4.29	Pressure Coefficient around cylinder at Re=150000	34
4.30	Vectors of Pressure Coefficient at Re=200000	34
4.31	Pressure Coefficient around cylinder at Re=200000	34
4.32	Vectors of Pressure Coefficient at Re=250000	35
4.33	Pressure Coefficient around cylinder at Re=250000	35
4.34	Vectors of Pressure Coefficient at Re=300000	35
4.35	Pressure Coefficient around cylinder at Re=300000	36
4.36	Vectors of Pressure Coefficient at Re=350000	36
4.37	Pressure Coefficient around cylinder at Re=350000	36
4.38	Strouhal Number vs Reynolds Number	38
4.39	Strouhal Number at Re=70000	38
4.40	Strouhal Number at Re=150000	38
4.41	Strouhal Number at Re=200000	39
4.42	Strouhal Number at Re=250000	39
4.43	Strouhal Number at Re=300000	39
4.44	Strouhal Number at Re=350000	40
4.45	Frequencies of Vortex Shedding vs Reynolds Number	41
4.46	Period vs Reynolds Number	41
B.1	Frequency at 70 000 Re, extracted directly from analysis figure	51
B.2	Frequency at 150 000 Re, extracted directly from analysis figure	52
B.3	Frequency at 200 000 Re, extracted directly from analysis figure	53
B.4	Frequency at 250 000 Re, extracted directly from analysis figure	54
B.5	Frequency at 300 000 Re, extracted directly from analysis figure	55
B.6	Frequency at 350 000 Re, extracted directly from analysis figure	56

## List of Tables

4.1	Pressure Coefficient for different Reynolds Number	37
4.2	Strouhal Number at different Reynolds Number	37
4.3	Calculated of Frequencies of Vortex Shedding and Period	40
A.1	Data of Analysis	47



## List of Appendices

<b>A</b>	<b>Frequency of Vortex Shedding</b>	<b>47</b>
<b>B</b>	<b>Figure of Frequency</b>	<b>49</b>

## List of Symbols

2D	Two-dimensional
3D	Three-dimensional
$\Gamma$	Diffusion coefficient
$\Delta t$	Time-step
$\varepsilon$	Turbulence dissipation rate
$\mu$	Dynamic viscosity (Ns/m <sup>2</sup> )
$\rho$	Fluid density (kg/m <sup>3</sup> )
$\omega$	Specific dissipation rate
$C_{\mu}$	Empirical constant
$C_d$	Drag coefficient
CFD	Computational Fluid Dynamics
CWT	Cooperative Wind Tunnel
D,d	Diameter (m)
DNS	Direct Numerical Simulation

f	Frequency
$F_o$	Vortex shedding frequency
FDM	Finite Difference Method
FEM	Finite Element Method
FIV	Flow-Induced Vibration
FVM	Finite Volume Method
I	Turbulence intensity
k	Kinetic energy
LES	Large Eddy Simulation
Re	Reynolds number
SST	Shear Stress Transport
St	Strouhal number
U	Fluid velocity (m/s)
$U_\infty$	Free stream velocity
$U_{avg}$	Mean flow velocity
VIV	Vortex-Induced Vibration

# Chapter 1

## Introduction

This chapter discussed about the CFD Simulation of Vortex-Induced Vibration of the Bluff Bodies Structure by ANSYS Fluent. The chapter consists of the background study, the problem statement, the objectives and the scopes of study. In the background study, the reader is then introduced to the CFD's Simulation, the vortex-induced vibration (VIV), the bluff bodies and the ANSYS Fluent software's.

### 1.1 Background of Study

In designing of a structure or structures, vibration of a structure is an important issue to encounter with. A structure could lead to a fatigue damage which is caused by vibrations. The environmental loading, either on the ground such as wind, or sea underneath such as waves and currents, are the main cause of the vibration.

In recent years, the study of flow around a bluff body becoming an important study, to investigate the effect of the flow induced vibration [1]. Its effect is relevant in designing, an on the ground structures such as taller buildings, bridges and other similar structures. Its effect also relevant in designing sea underneath structures such as pipelines and risers.

### 1.1.1 Vortex-Induced Vibration

Vibration phenomenon which occurs to the bluff body structure, either on the ground or sea underneath could be regarded as vortex-induced vibration (VIV). Previous researchers have been widely discussed in both detail and comprehensive ways to understand the vortex-induced vibration mechanism from a bluff body [2,3].

As the flow passed a bluff body at a sufficiently large Reynolds number, vortices would be shedding at the trailing edge of the body. A fluctuating lift force, was created due to the pressure difference on the side of the body surface which eventually would create cross-flow vibrations.

The source of vibration was from the vortex formed that occurs after the flow passed a bluff body structure. Large amplitude vibration phenomenon would strike if the frequency of the vortex shedding and approaching the natural frequency of the bluff body structure.

These large amplitudes vibration phenomena were also called lock-in [1]. This type of fluid-structure interaction problem has been widely investigated numerically and experimentally in the past.

### 1.1.2 Bluff Body

There were two types of shape's structure which were that streamline shape and non-streamline shape. The streamline shapes often called aerodynamic body while the non-streamline shape often called bluff body.

As a result of its shape, a bluff body separated, flow over a substantial part of its surface. An important feature of a bluff body flow is that there is a very strong interaction between the viscous (significant to the frictional effect because of the viscosity) and inviscid (ideal fluid that is assumed to have no viscosity) regions [4,5]. Examples of bluff bodies include circular cylinders, square cylinders and rectangular cylinders.

### 1.1.3 Computational Fluid Dynamics (CFD)

CFD calculates numerical solutions to the equations governing fluid flow. As opposed to flow around a streamlined body, bluff bodies were the structures with shapes that significantly disturb the flow around them.

To model the fluid-structure interaction, the CFD software ANSYS Fluent 14 was used to predict the results around cylindrical bluff body at each time step. The cylindrical bluff body structured was tested at a difference Reynolds number. The predicted results around the cylindrical bluff body are validated through previous journals results.

## 1.2 Problem Statement

At low flow velocities, the fluid flow around the cylindrical bluff body acts as a damper, limiting the amplitude of motion. The investigations of the effect of flow velocity on the transverse vibration of bluff body were done to determine the vortex shedding frequency for each of the analyses. Besides it was also done to investigate the flow velocity and pressure loss in the time response.

However, as the flow velocity increased, the pressure and shear forces also increased, which increased the net lift and drag forces on the cylindrical bar. Eventually, at some critical velocity, the energy input from these external fluid forces exceeds the structural damping and the amplitude of the cylindrical bluff body vibration rises dramatically, particularly in the cross-flow direction. Despite the investigation made by other researchers, a study on a very high turbulence Reynolds number, were still blurred unknown.

In response to this problem, this study proposed to investigate several options such as increasing the Reynolds number. The turbulence studied started from a minimum of 70 000 Reynolds number and increased to the maximum of 350 000 Reynolds number.

## 1.3 Objective of the Study

The aim of this study was:

1. To investigate the effect of flow velocity on the transverse vibration of bluff body.
2. To determine the Strouhal number for each of the analyses.
3. To determine the vortex shedding frequency for each of the analyses.

## **1.4 Scopes of the Study**

The scopes for this study were:

1. Aluminium cylindrical shape with one meter of diameter.
2. Shape is allow to move in cross-flow direction
3. Test at different Reynolds Number which were 70 000 Re, 150 000 Re, 200 000 Re, 250 000 Re, 300 000 Re and 350 000 Re.
4. Time independent test (non-steady, transient)

## Chapter 2

### Literature Review

This chapter discussed about the work of past researchers. This chapter would discuss about the Reynolds number, the Strouhal number, the effect of flow velocity, the vortex shedding and the previous work of research. In the previous research, several sub-topics will be discussed such as, the methodology, results and discussion and finally the conclusion of previous research.

Fluid flowed behaviour could be analysed throughout the experiment and empirical studies. To study the characteristics of the fluid flows, several tests had been conducted. Differential equations and mathematical relations were used to obtain new equations. Experimental and numerical method was always used as the methods to investigate the fluid behaviour.

To solve the numerical equations, a program called Computational Fluid Dynamics (CFD) was developed. Throughout the development of CFD, numbers of fluid problem were solved, although it was a complicated problem. Vortex shedding was one example of the complicated problems, which need to be solved computationally.

For many decades, vortex shedding from the bluff bodies has been always a main subject that attracted many researchers to study and investigate. A high tower building, for example, is the significance of the periodic unsteady fluid flows which passed from bluff bodies. Vibrations near the bluff body were produced by the vortices which may be dangerous to the structure.



## 2.1 Reynolds Number

One of the very important non-dimensional numbers was the Reynolds Number (Re) [3-9]. It is used in predicting flow patterns in different fluid flow situations. The Reynolds number expresses the ratio of inertial (resistant to change or motion) forces to viscous (heavy and gluey) forces [2]. Reynolds number determines dynamic similitude between two different cases of fluid flow.

Reynolds Number is given by the formula,

$$Re = \frac{\rho U D}{\mu} \quad (2.1)$$

where  $\rho$  is the fluid density (kg/m<sup>3</sup>),  $U$  is the velocity based on the actual cross area of the duct or pipe (m/s),  $D$  is the pipe diameter (m) and  $\mu$  is the dynamic viscosity (Ns/m<sup>2</sup>).

Besides that, Reynolds number also used to characterize different flow regimes within a similar fluid, such as laminar flow or turbulent flow. Laminar flow is characterized by smooth and constant fluid motion. Laminar flow occurs at low Reynolds numbers, where viscous forces were the dominant. Turbulent flow occurs at high Reynolds numbers and is dominated by inertial forces. Turbulent flow produces chaotic eddies, vortices and other flow instabilities.

## 2.2 Strouhal Number

Another important non-dimensional number was the Strouhal number (St) [4-9]. The Strouhal number is used to analyse the unsteady-state, oscillating flow problems [10].

Strouhal number, defined as a ratio of inertial forces due to the unsteadiness of the flow or local acceleration to the inertial forces due to changes in velocity from one point to another in the flow field [10].

Strouhal Number is given by the formula,

$$St = \frac{f D}{U} \quad (2.2)$$

where  $f$  is the characteristic oscillation frequency,  $D$  is the characteristic length and  $U$  is the velocity of the fluid.

## 2.3 Effect of Flow Velocity

Several factors such as force components, shedding frequency, Reynolds number, material damping and structural stiffness of the cylinder, were the caused that affected the vortices to generate [11].

As the Reynolds number increases, the amplitude as well as the frequency of the velocity signals also increases. An increase in Reynolds number causes an increase in the Strouhal frequency of a single bluff body and for a row of bluff bodies [12].

## 2.4 Vortex Shedding

When shedding vortices (a Von Karman vortex street) exert oscillatory forces on a cylinder in the direction perpendicular to both the flow and the structure, a vortex-induced vibration (VIV) occurs [11].

When a solid and fluid interact, the instabilities appearing in flow fields induce instabilities in the neighbouring solid structures [12]. Special emphasis is required to analyse the VIV because vortex shedding and wake dynamics or flows passed bluff bodies were a complex flow problem [2, 12].

When cylinders with a bluff cross section, immersed in a free stream with their axis perpendicular to the flow, they were susceptible to a range of flow-induced vibration (FIV) phenomenon [13]. For circular cylinders, which do not have a defined angle of attack, the phenomenon of VIV is more likely to occur, which is due to periodic vortex shedding in the wake [13].

The periodic shedding was where a vortex was shedding from one side of the body, and then a vortex of opposite sign was shedding from the other side of the body and forms the Karman vortex street [13]. Large-amplitude oscillations can occur in the resonance-type response when the vortex shedding frequency is close to a natural structural frequency [13]. The vortex shedding frequency

also would change to match with the body oscillation frequency, which leading to large, periodic oscillations.

## 2.5 Previous Research

Rahman et.al [14] investigates unsteady flow passed a circular cylinder using a 2D finite volume method with different Reynolds number.

Vijaya et.al [15] studied 2D unsteady flows of power-law fluids over a cylinder. The study has been solved using a finite volume method based solver FLUENT 6.3.

Mittal and Kumar [2] studied VIV on a pair of equal-size cylindrical cylinders with two sets of arrangement, inline and staggered. The fixed cylinders for the 2D simulation were simulated in a rectangular computational domain with a fixed Reynold number,  $Re = 1000$ .

Shao and Zhang [4] used the finite volume method to investigate two side-by-side cylindrical cylinders. The cylinders were simulated in a 23 times of the cylinder diameter computational domain with a constant inlet velocity  $U_8 = 7\text{m/s}$ . Second orders implicit temporal discretization with a time step of  $\Delta t = 1 \times 10^{-4}$  s was used.

Bourguet et.al [6] studied lock-in of the VIV on an in-line flow of a flexible cylindrical cylinder using direct numerical simulation (DNS) of the 3D incompressible Navier-Stokes equations.

Pratish and Tiwari [12] investigate unsteady wakes behind two inline arrangement of square cylinders. 2D computational domain was used where the length and width of the channel were 16 times and 6 times of the square width cylinders.

Chandrakant and Swapnil [16] analyzed vortex shedding behind a D-shaped cylinder. 2D computational domain with 2 m length and 1.6 m and quad meshing was used for the study.

Ali and Edris [17] analyzed the numerical simulation of unsteady flow with vortex shedding around circular cylinder. Two-dimensional flow of an incompressible fluid around a circular cylinder were simulated in both uniform

stream flow and oscillated flows at  $Re=300$ . The computational domain with length, 0.3m and width, 0.2m with water as the assumption liquid was used in the study.

Roshko [18] conducted an experiment on the flow passed a circular cylinder at a very high Reynolds number. The experiments were conducted in the Cooperative Wind Tunnel (CWT) in the subsonic test section of 2.591m height and 3.353m width which could be pressurized to 4 atm, but to avoid compressibility effects, the flow speed was limited to a Mach number of 0.25 or 85.07 m/s. The arrangement was shown in Figure 2.1.

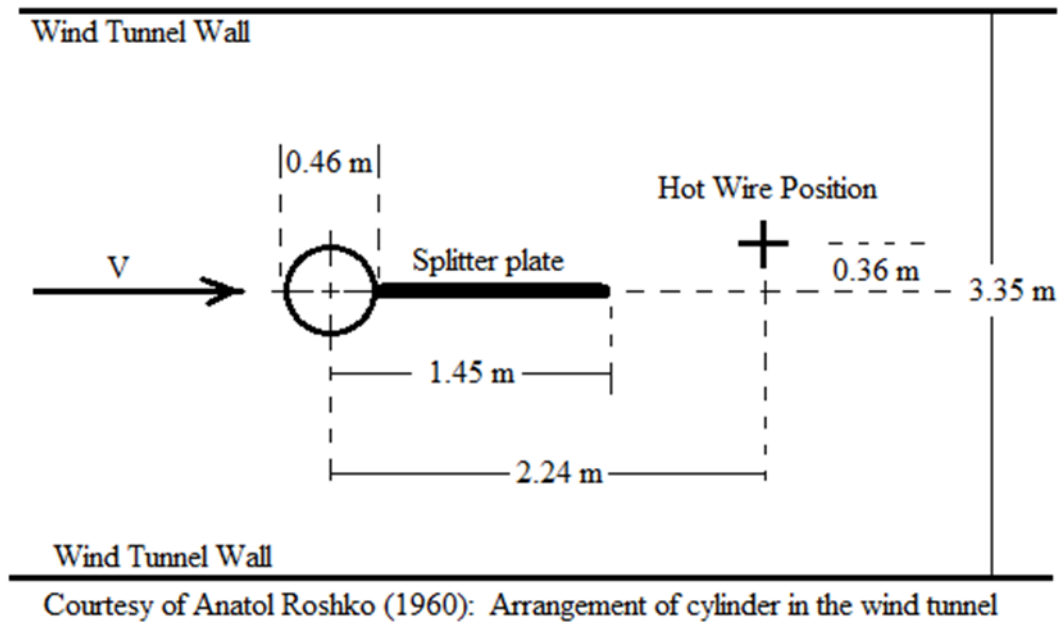


Figure 2.1: Cylinder arrangement in the wind tunnel

Rahman et.al [14] found that, as Reynolds number becomes higher than 40 the flow reports a loss of symmetry in the wake. The studied also reported the Strouhal number ( $St$ ) is found to be 0.164 for  $Re=100$ .

Mittal and Kumar [2] reported the non-dimensional value of the vortex shedding frequency is  $F_o = 0.234$  for both cylinders while the non-dimensional frequency corresponding to the cross-flow oscillations of both cylinders is 0.226.

Chandrakant and Swapnil [16] reported that the Strouhal number increases with increase in Reynolds number and the number of vortices increases with Reynolds number.

Ali and Edris [18] reported the computed drag coefficient ( $C_d$ ) and the Strouhal number in four numbers of nodes. For the number of nodes 28 000, 57 500, 82 500 and 103 000, the  $C_d$ s were 1.345, 1.353, 1.366 and 1.366 while the Strouhal numbers were 0.202, 0.204, 0.207 and 0.207.

Roshko [13] found out that vortex shedding was not observed at  $Re < 3.5 \times 10^6$ . Below the value of  $Re < 3.5 \times 10^6$ , no peak frequency occurred, but above this value there appeared a strong spectral peak, said to be well above the turbulence level.

Rahman et.al [14] observed that standard k-epsilon model computes drag coefficients accurately. The realizable k-epsilon turbulence model is more effective for visualization of vortex shedding, while for the SST k-omega model, it is recommended for high Reynolds numbers.

Mittal et.al [2] concluded that the oscillations of the cylinders result in an alternate mode of vortex shedding and where the vibration of cylinders is usually accompanied by an increase in drag.

Shao et.al [4] concluded that LES is capable of reproducing complex subcritical turbulent wake behind a circular cylinder, but fine meshes and longer time were required for the flow around the circular cylinder.

Bourguet et.al [6] concluded that the structural vibrations are mixtures of standing and traveling wave patterns. A frequency ratio of approximately 2 can be established between the excited frequencies in the in-line and cross-flow directions.

Mittal et.al [2] concluded that for a circular cylinder, flow separation point changes with Reynolds number, so the wake is unsteadiness.

## **Chapter 3**

### **Methodology**

This chapter discussed about the methodology of this present work. This chapter started with an introduction followed by physical model. In the physical model, previous model has been chosen as a present model with some modification. The numerical methods would discuss on discretization methods such as FVM, FEM and FDM. This chapter also consists of the governing equation and the boundary conditions of the present study based on previous study. In the CFD, it would discuss on the process involved, such as preprocessing, solver and post-processing.

#### **3.1 Numerical Study**

This numerical study was carried out to investigate the effect of flow velocity on the transverse vibration of bluff body in the CFD, together with the effects of variation of the Reynolds number.

Obviously, the Reynolds number was an important non-dimensional number to determine the types of flow, either laminar or turbulent flow. Most flows were turbulent in nature and it was applied in engineering too. Turbulence was the chaotic nature of flow in motion showing random variation in space and time.

Turbulence, contains eddies with different scales and sizes. These eddies were always rotational in motion. Large scale eddies were responsible for the carrying of energy and transfer of momentum in the flow. The large eddies, extract energy from the mean flow and transfer it to the smallest eddies, where

energy was taken out of the flow through viscosity.

The well-known equations of fluid motion were known as the Navier-Stokes equations. These equations have been derived based on the fundamental governing equations of fluid dynamics. These fundamental was the continuity, the momentum and the energy equations, which represent the conservation laws of physics.

Continuity equation was based on the law of conservation of mass. Once the concept applied to the fluid flow, the change of mass in a control volume was equal to the mass that enters through its faces minus the total of mass leaving its faces.

Momentum equation was expressed in terms of the pressure and viscous stresses. Both pressure and viscous, stresses acting on a particle in the fluid. This would ensure that the rate of change of momentum of the fluid particles was equal to the total of the force. This was due to the surface stresses and body forces.

The energy equation was based on the First Law of Thermodynamics. The rate of change of energy of a fluid particle was to be equal to the net rate of work has done on that particle. This was due to surface forces, heat and body forces such as gravitational force. The energy equation describes the transport of heat energy through a fluid and its effects.

A Navier-Stokes equation was a set of partial differential equations, with the combination of all those fundamental principles which was the continuity, momentum and energy equations. Pressure and velocity of the fluid can be predicted throughout the flow by solving these equations.

## 3.2 Physical Model

The physical modelled that used in this study was similar to the physical studied by Rahman et.al [7]. A circular cylinder with diameter,  $d$ , was modelled in the centre with a square flow domain is created surrounding the cylinder as shown in Figure 3.1.

The computational domain for an upstream was 23 times of the circular cylinder radius while for the downstream was 40 times the radius of the circular

cylinder. The width of the domain was 50 times the radius of the circular cylinder which was shown in Figure 3.1 together with the important dimensions [7].

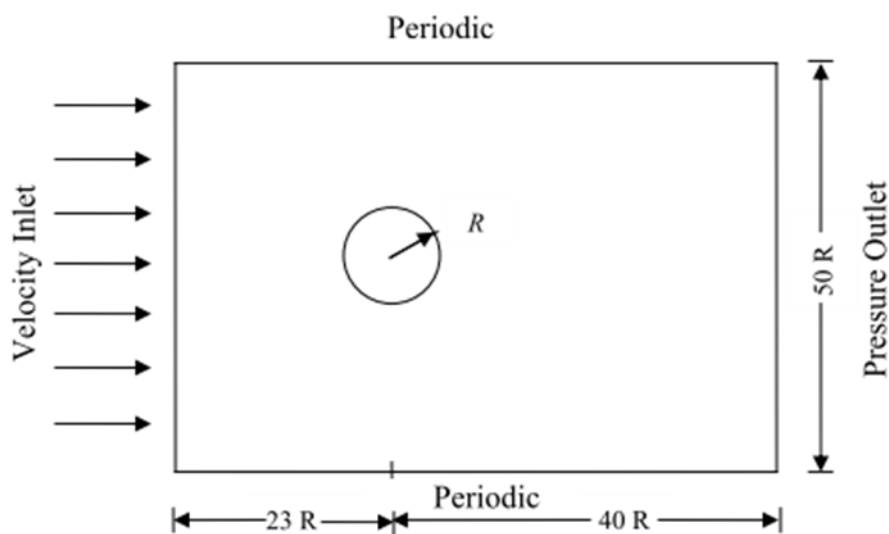


Figure 3.1: Schematic diagram of the flow field around circular cylinder [7]

### 3.3 Numerical Methods

To solve the engineering problems, besides analytical and experimental methods, the ability of numerical methods in fluid mechanics has increased. The used of the numerical methods was to find numerical approximations to the solutions where most of the differential equations could not be solved exactly.

In the Computational Fluid Dynamics (CFD), Navier-Stokes equations were the basic governing equations. The equations were obtained by applying Newton's Law of Motion to a fluid element. It was also called as the momentum equation, and supplemented by the mass conservation equation which was also called the continuity equation and energy equation.

CFD was used to construct and discretise the governing equations, through discretisation methods such as Finite Difference Methods (FDM), Finite Element Methods (FEM) and Finite Volume Methods (FVM).



### 3.3.1 Finite Volume Method

In a steady state solution the inlet and outlet mass flow rate would be obtained equally. The change of momentum would equal the force exerted on solid boundaries. The solution of the steady state problems is performed by starting from an arbitrary initial guess of the flow field and marching the equations forward in time until the flow becomes steady. If the flows entered and left every volume were not equal, the conditions inside the volume must be changed and the flow was not steady anymore.

Even the flow was at steady, the used in unsteady equations was found to be very useful to solve the engineering problems. The FVM was based on the discretisation of the Navier-Stokes equations. Every volume was contiguous with its adjacent volumes, and that the flow from recent volumes will enter the adjacent volumes, and therefore, when a steady state reached, the flow was fully utilized.

### 3.3.2 Finite Element Method

The Galerkin method was most commonly used formulation in FEM in fluid mechanics. The Galerkin method employs weighted residuals whereby their form was usually assumed similar to the shape functions. The Galerkin method approximates the solution in terms of unknown nodal, and interpolated by the shape functions.

### 3.3.3 Finite Difference Method

The conservation equations in differential form were approximated by replacing the partial derivatives by approximations in terms of the nodal values of the functions. Taylor series expansions or polynomial fitting were usually used to obtain the derivatives of the functions with respect to the coordinates. This yields an algebraic equation for each grid node in which values of neighbouring nodes appear as unknowns. Although theoretically possible for unstructured grids, FDM have only been applied to structure grids.

### 3.4 Governing Equations

The mathematical model of the finite volume method (FVM) that was used in this study was similar to the model of numerical investigation of unsteady flow passed a circular cylinder, studied by Rahman et.al [7]. The governing equations for the unsteady flow of an incompressible viscous fluid passed a circular cylinder were considered to the classical continuity and Navier-Stokes equations, which written in the following form:

$$\text{div}(\vec{u}) \quad (3.1)$$

$$\frac{\partial(u)}{\partial t} + \text{div}(u\vec{u}) = \frac{1}{\rho} \text{div}(\Gamma \nabla u) \quad (3.2)$$

On the left side of the equation (3.2) was the rate of change term and the convective term and on the right side was the diffusion term,  $\Gamma$  = diffusion coefficient which was used as the starting point in FVM.

$$\int_{cv} \frac{\partial(u)}{\partial t} dv + \int_{cv} \text{div}(u\vec{u}) dv = \frac{1}{\rho} \int_{cv} \text{div}(\Gamma \nabla u) dv \quad (3.3)$$

In the second term of the left hand side of the equation (3.3) was the convective term and on the right side was the diffusion term. By using the Gauss divergence theorem, it could be rewritten as an integral over the entire boundary surface of the control volume and the equation (3.3) became

$$\frac{\partial}{\partial t} \left[ \int_{cv} (u) dv \right] + \int_A n. (u\vec{u}) dA = \frac{1}{\rho} \int_A n. (\Gamma \nabla u) dA \quad (3.4)$$

The rate of change term was equal to zero in the steady state case and the equation (3.4) became

$$\int_A n. (uU) dA = \frac{1}{\rho} \int_A n. (\Gamma \nabla u) dA \quad (3.5)$$

For the unsteady (time dependent) case it was necessary to integrate with respect to time,  $t$ , over a small time interval,  $\Delta t$  i.e. from  $t$  to  $t + \Delta t$ , Equation (3.5) became

$$\int_{\Delta t} \frac{\partial}{\partial t} \left[ \int_{cv} (u) dv \right] dt + \int_{\Delta t} \int_A n. (u\vec{t}) dA dt = \frac{1}{\rho} \int_{\Delta t} \int_A n. (\Gamma \nabla u) dA dt \quad (3.6)$$

In FVM, flow domain was divided into a number of control volumes or cells which was called discretization. In order to solve the problem, equation (3.6) needs to be discretized to be set up at a nodal point.

The resulting system of linear algebraic equations was then solved to obtain the velocity and pressure distribution at each nodal point. Finally, the drag and the lift coefficients were computed as follows:

$$C_D = \frac{D}{0.5U_\infty^2 d}, C_{DP} = \int_0^{2\pi} P_w \cos x dx, C_{DV} = \frac{2}{Re} \int_0^{2\pi} \omega_w \sin x dx \quad (3.7)$$

$$C_L = \frac{D}{0.5U_\infty^2 d}, C_{LP} = \int_0^{2\pi} P_w \sin x dx, C_{LV} = \frac{2}{Re} \int_0^{2\pi} \omega_w \cos x dx \quad (3.8)$$

Where, D and L represent the drag and lift force. The pressure coefficient was defined as:

$$C_P = \frac{(P - P_\infty)}{0.5\rho U^2 d} \quad (3.9)$$

The subscripts P and V represent the pressure and viscous force.  $P_w$  is the dimensionless wall pressure and  $\omega_w$  is the dimensionless wall vorticity, defined as

$$\omega_w = \frac{\omega R}{U_\infty}, R = 0.5 \quad (3.10)$$

The dimensionless Reynolds number was given by:

$$Re = \frac{dU_{\infty}\rho}{\mu} \quad (3.11)$$

The Strouhal number was expressed as:

$$St = \frac{fD}{U_{\infty}} \quad (3.12)$$

Where, the frequency of the vortex shedding,  $f$  ( $=1/T$ ), the diameter of the cylinder,  $d$ , and the free stream velocity,  $U_{\infty}$ .

The viscous forces of the turbulent flow were suggested to use standard  $k-\epsilon$ , realizable  $k-\epsilon$  and Shear-Stress Transport (SST) as suggested by Lakshmiopathy [7]. The standard  $k-\epsilon$  model was based on model transport equations for the turbulence kinetic energy ( $k$ ) and its dissipation rate ( $\epsilon$ ) [7].

In the derivation of the  $k-\epsilon$  model, it was assumed that the flow is fully turbulent, and the effects of molecular viscosity are negligible. The standard  $k-\epsilon$  model is therefore valid only for fully turbulent flows [7]. The turbulent kinetic energy,  $k$ , was given by:

$$k = \frac{3}{2}(U_{avg}I)^2 \quad (3.13)$$

Where,  $U_{avg}$  was the mean flow velocity and  $I$  was the turbulence intensity. The turbulence intensity,  $I$ , was defined by:

$$I = 0.16(Re)^{\frac{1}{8}} \quad (3.14)$$

The turbulence length could be written as  $l=0.07d$  and the turbulence dissipation rate,  $\epsilon$ , as,

$$\epsilon = U_{\mu}^{\frac{3}{4}} \frac{k^{\frac{3}{2}}}{l} \quad (3.15)$$

where  $C_{\mu}$  was an empirical constant, specified in the turbulence model,

which was approximately 0.09.

SST k- $\epsilon$  was another turbulent model, but modified to use with shear stress turbulent [7]. The specific dissipation rate,  $\omega$ , in the modify SST k- $\epsilon$  could be found by,

$$\omega = \frac{k^{\frac{1}{2}}}{C_{\mu}^{\frac{1}{4}} l} \quad (3.16)$$

### 3.5 Boundary Conditions

The uniform flow condition was imposed at the inlet boundary while pressure was treated at the outlet boundary. The standard no-slip condition was used on the surface of the cylinder, which was  $U_x = 0$  and  $U_y = 0$ . At the top and bottom wall boundaries, the slip-flow condition was imposed where,

$$\frac{\partial U_x}{\partial y} = 0 \text{ and } U_y = 0 \quad (3.17)$$

### 3.6 Computational Fluid Dynamics

The investigation performed on the wake properties of the two dimensional flow and a cylindrical bluff body by using the finite volume method. By using a computer, the CFD solves the Navier-Stokes equations numerically for fluid flow.

Graphs and charts in CFD were used to analyze the flow characteristics in order to compare with the previous researchers' results. This study was performed in three steps, which were pre-processing, solver and post-processing by ANSYS Fluent R14. Those steps were shown in Figure 3.2.

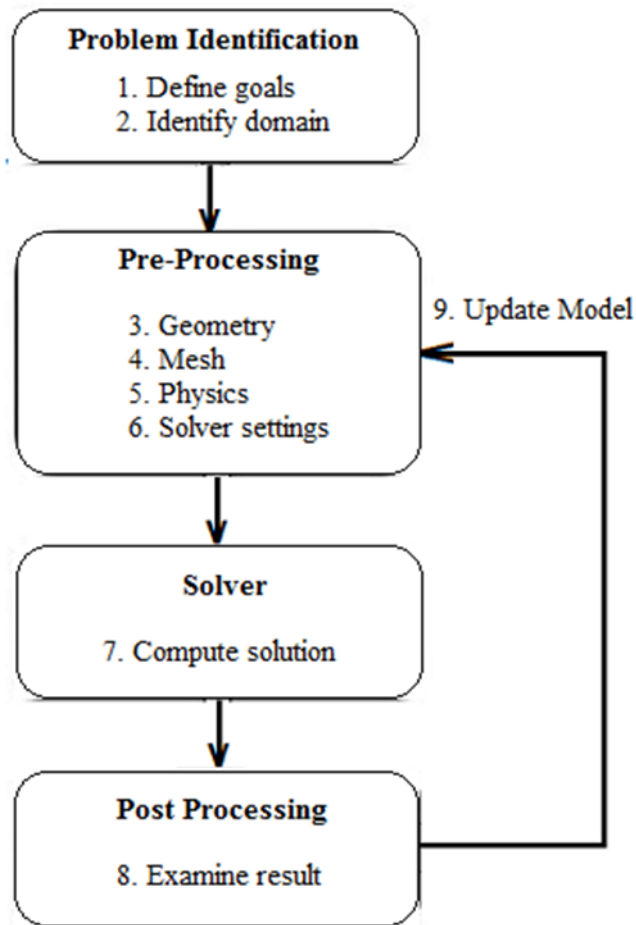


Figure 3.2: Steps Performed in CFD

### 3.6.1 Preprocessing

After creating a solid model of the domain, the first step of the CFD simulation process was the pre-processing which will describe the geometry in detailed. The domain of interest is then further divided into smaller segments which were known as meshed.

The properties of the fluid acting on the domain need to be defined first before begin the analysis. These include external constraints or boundary conditions, like pressure and velocity to implement realistic situations.

### **3.6.2 Solver**

A solver calculates the solution of the CFD problem where the governing equations were solved. Identified physical problem such as fluid material properties, flow physics model and boundary conditions were set to solve using a computer. It was important to produce an accurate solution of the partial differential equations by doing the convergence.

### **3.6.3 Post Processing**

Flow phenomena would be presented in different methods, such as contour plots, vector plot, streamlines, data curve and others related to the study. All those methods would be used to analyze the results for appropriate graphical representations to display the trends of velocity, pressure, kinetic energy and other properties of the flow.

## **3.7 Methodology Summary**

The methodology would be much better if it could be summarized. Therefore a summarized methodology was clearly shown in a flowchart type as in Figure 3.3.

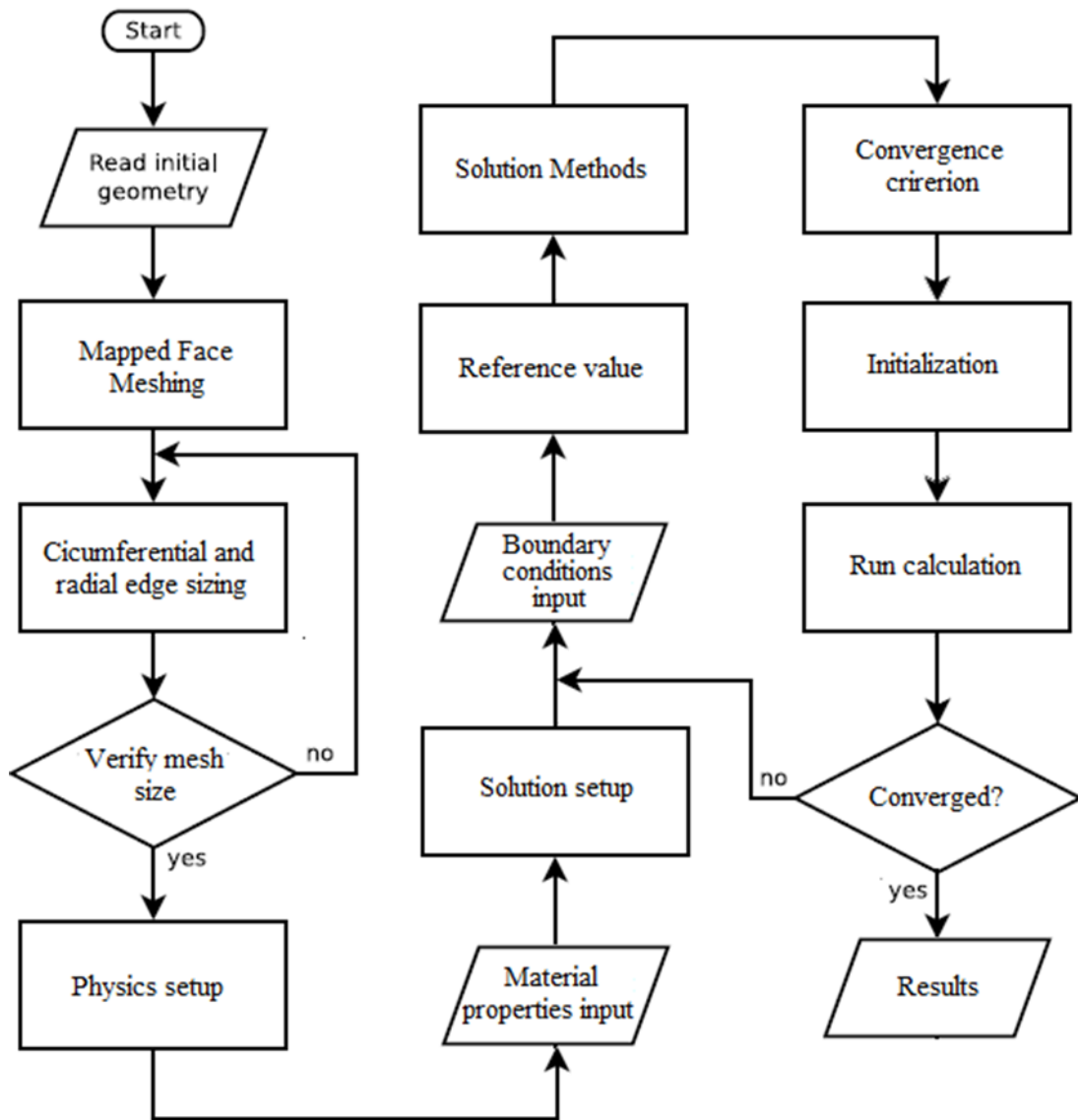


Figure 3.3: Flowchart of Methodology



## Chapter 4

### RESULTS AND DISCUSSION

This chapter discussed the extracted results of the cylindrical simulation. The simulation was done in the flow of turbulence. The turbulence flow was ranged from  $70\,000 < Re < 350\,000$ . The results were analysed through the contours and vectors of velocity and pressure coefficient figures. The Strouhal Number was determined throughout the use of Strouhal figures, extracted from the analysis.

#### 4.1 Validation

In order to validate, data's from Simmons which was used by Roshko [13] had been chosen. From the trend pattern, the extracted simulated data's was then satisfied as we could see as shown in the Figure 4.1.

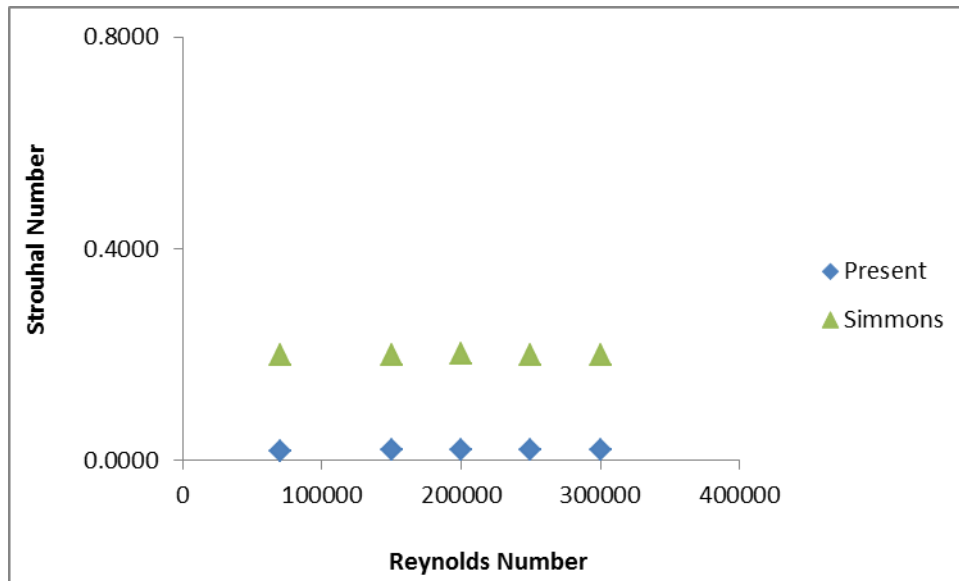


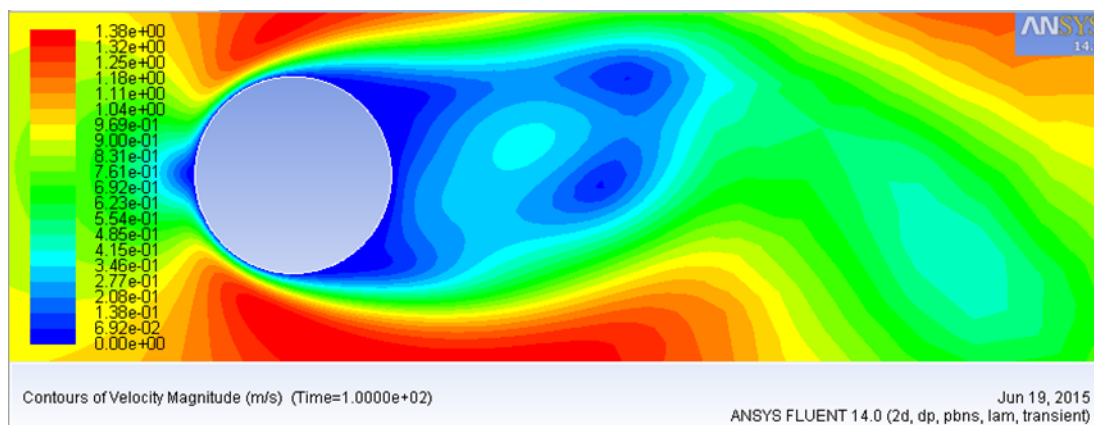
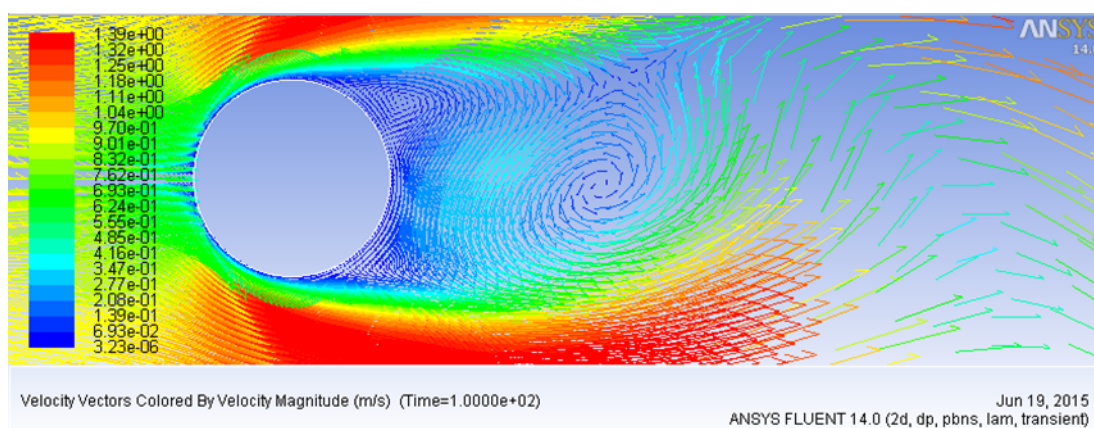
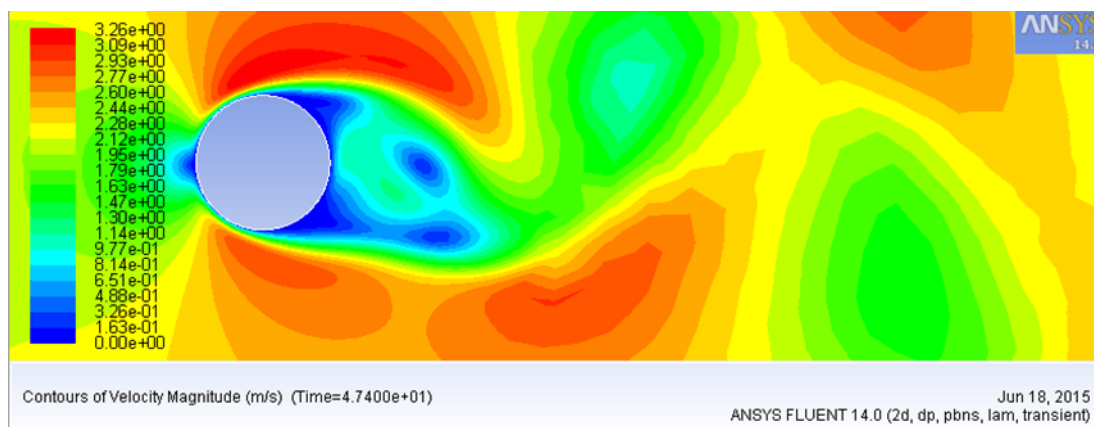
Figure 4.1: Trending line validation between present study and Simmons

## 4.2 Velocity Magnitude

It could be seen as from Figure 4.2 to 4.13, the fluid flow after the boundary layer at high Reynolds Number was an asymmetric flow. The vortex shedding is visualized throughout the contours and vectors of velocity magnitude.

As seen from the Figure 4.2 to 4.13, as the flow stream past the cylinder, vortices were formed behind the cylinder. From all those figures, it could be seen, as the flow speed increased, vortices were alternately shed on each side.

The vortex shedding clearly observed in all those figures and it could be stated clearly that the vortex shedding proportional to the velocity magnitude which was also proportional to the Reynolds Number.

Figure 4.2: Contours of Velocity Magnitude at  $Re=70000$ Figure 4.3: Vectors of Velocity Magnitude at  $Re=70000$ Figure 4.4: Contours of Velocity Magnitude at  $Re=150000$

## Chapter 5

### CONCLUSIONS AND RECOMMENDATIONS

From the research of simulation of Vortex Induced Vibration, the investigated effect of flow velocity could be observed from the pressure coefficient and vorticity magnitude.

It could be seen the increases of velocity which would also increase the Reynolds number where the fluid flow past a bluff body creates vortices and were alternately shed on each side.

The vortex shedding frequencies were determined throughout the extracted results and data's of the Strouhal number. It could be concluded, the Strouhal numbers decreased with the increased of Reynolds number.

For the Reynolds number of 70 000 Re, 150 000 Re, 200 000 Re, 250 000 Re, 300 000 Re and 350 000 Re the Strouhal number were 0.017, 0.0194, 0.020, 0.0195, 0.0192 and 0.0184.

For the frequencies of vortex shedding, it could be concluded the increased of Reynolds number would increase the frequencies while for the period or duration of one cycle, decreased with the increased of Reynolds number.

For the Reynolds number of 70 000 Re, 150 000 Re, 200 000 Re, 250 000 Re, 300 000 Re and 350 000 Re the frequencies were 0.0174, 0.0425, 0.0584, 0.0712, 0.0841 and 0.094.

For the future work, there were still gaps that left behind in this research. It could be recommended for the future research to study on different turbulence model and different material.

## References

- [1] M. T. Asyikin, CFD Simulation of Vortex Induced Vibration of a Cylindrical Structure, Norwegian University of Science and Technology, Trondheim, 2012.
- [2] S.Mittal and V.Kumar, Vortex Induced Vibrations of a Pair of Cylinders at Reynolds Number 1000, International Journal of Computational Fluid Dynamics, vol. 18(7), p. 601-614, 2004.
- [3] X. Wang, B. Su and B. Su, Experimental study of vortex-induced vibrations of a tethered cylinder, Journal of Fluids and Structures, vol. 34, pp. 51-57, 2012.
- [4] J. Shao and C. Zhang, Large eddy simulations of the flow past two side-by-side circular cylinders, International Journal of Computational Fluid Dynamics, vol. 22(6), p. 393-404, 2008.
- [5] H. Aref, M. Stremmer and F. Ponta, Exotic vortex wakes—point vortex solutions, Journal of Fluids and Structures, vol. 22, p. 929-940, 2006.
- [6] R. Bourguet, G. E. Karniadakis and M. S. Triantafyllou, Lock-in of the vortex-induced vibrations of a long tensioned beam in shear flow, Journal of Fluids and Structures, vol. 27, pp. 838-847, 2011.
- [7] Z. Pan, W. Cui and Q. Miao, Numerical simulation of vortex-induced vibration of a circular cylinder at low mass-damping using RANS code, Journal of Fluids and Structures, vol. 23, p. 23-37, 2007.
- [8] S. Manzoor, J. Khawar and N. A. Sheikh, Vortex-Induced Vibrations of a Square Cylinder with Damped Free-End Conditions, Advances in Mechanical Engineering, vol. 5, 2013.

- [9] F. Ponta and H. Aref, Numerical experiments on vortex shedding from an oscillating cylinder, *Journal of Fluids and Structures*, vol. 22, p. 327-344, 2006.
- [10] M. Dular and R. Bachert, The Issue of Strouhal Number Definition in Cavitating Flow, *Journal of Mechanical Engineering* , vol. 55, pp. 666-674 , 2009.
- [11] R. Gabbai and H. Benaroya, An overview of modeling and experiments of vortex-induced vibration of circular cylinders, *Journal of Sound and Vibration*, vol. 282, p. 575-616, 2005.
- [12] P. P. Patil and S. Tiwari, Numerical Investigation of Laminar Unsteady Wakes Behind Two Inlinw Square Cylinders Confined in a Channel, *Engineering Applications of Computational Fluid Mechanics*, vol. 3(3), p. 369-385, 2009.
- [13] J. S. Leontini and M. C. Thompson, Active control of flow-induced vibration from bluff-body wakes: the response of an elastically-mounted cylinder to rotational forcing, in 18th Australasian Fluid Mechanics Conference, Launceston, Australia, 2012.
- [14] M. M. Rahman, M. M. Karim and M. A. Alim, Numerical Investigation of Unsteady Flow Past a Circular Cylinder using 2-D Finite Volume Method, *Journal of Naval Architecture and Marine Engineering*, vol. 4, p. 27-42, 2007.
- [15] V. K. Patnana, R. P. Bharti and R. P. Chhabra, Two-dimensional unsteady flow of power-law fluids over a cylinder, *Chemical Engineering Science*, vol. 64, pp. 2978-2999, 2009.
- [16] C. D. Mhalungekar and Swapnil.P.Wadkar, CFD and Experimental Analysis of Vortex Shedding behind D-shaped Cylinder, *International Journal of Innovative Research in Advanced Engineering*, vol. 1(5), 2014.
- [17] A. Kianifar and E. Y. Rad, Numerical Simulation of Unsteady Flow with Vortex Shedding Around Circular Cylinder, in *International Conference on Theoretical and Applied Mechanics 2010; International Conference on Fluid Mechanics and Heat & Mass Transfer 2010*, Corfu Island, Greece, 2012.
- [18] A. Roshko, Experiments on the flow past a circular cylinder at very high Reynolds number, *Journal of Fluid Mechanics*, vol. 10(3), pp. 345-356, 1960.

- [19] National Aeronautics and Space Administration (NASA), 12 Jun 2014. [Online]. Available: <http://www.grc.nasa.gov/WWW/BGH/reynolds.html#>.
- [20] B. Sunden, "Thermopedia," 16 March 2011. [Online]. Available: <http://www.thermopedia.com/content/1216/?tid=104&sn=1410>. [Accessed 16 December 2014].